Vallespir, F.; Carcel Carrión, JA.; Marra, F.; Eim, VS.; Simal, S. (2018). Improvement of Mass Transfer by Freezing Pre-treatment and Ultrasound Application on the Convective Drying of Beetroot (Beta vulgaris L.). Food and Bioprocess Technology. 11(1):72-83. https://doi.org/10.1007/s11947-017-1999-8

Improvement of mass transfer by freezing pre-treatment and ultrasound application on the convective drying of beetroot (*Beta vulgaris* L.)

Francisca Vallespir[a], Juan A. Cárcel[b], Francesco Marra[c], Valeria S. Eim[a], Susana Simal[a*]

[a] Department of Chemistry, University of the Balearic Islands. Ctra Valldemossa km 7.5, 07122 Palma de Mallorca, Spain.

[b] ASPA Group, Food Technology Department, Polytechnic University of Valencia, Cno Vera s/n, 46021 Valencia, Spain.

[c] Dipartimento di Ingegneria Industriale, Università degli Studi di Salerno, Via Giovanni Paolo II 132, 84084 Fisciano, SA, Italy.

* Corresponding author: Tel.: +34971172757. E-mail address: susana.simal@uib.es; Permanent address: Ctra Valldemossa km 7.5, 07122. University of the Balearic Islands Palma de Mallorca, Spain.

Abstract:

The effects of freezing pre-treatment and ultrasound application during drying on microstructure, drying curves and bioactive compounds of beetroot have been evaluated. Raw and previously frozen (at –20 °C) beetroots were convectively dried (40 °C and 1 m/s) with and without ultrasound application using two acoustic densities (16.4 kW/m^3 and 26.7 kW/m^3), and a diffusional model was proposed to simulate the drying curves. Freezing pre-treatment and ultrasound application caused significant disruptions in the beetroot microstructure and reduced the drying time, enhancing the mass transfer. The external mass transfer coefficient significantly ($p<0.05$) increased by 28-49% when ultrasound was applied; moreover, the effective diffusion coefficient significantly ($p<0.05$) increased by 60-73% and 204-211% respectively, due to the ultrasound application on the drying of raw and pre-frozen samples. Freezing caused significant ($p<0.05$) increases in betalain and total polyphenol contents and antioxidant activity compared with the raw sample (16-57%), probably due to the release of free forms from the food matrix, meanwhile drying had the opposite effect (8-54% decrease). Significantly ($p<0.05$) higher decreases (32-81%) in bioactive compounds and antioxidant activity were observed when drying was assisted by ultrasound compared with dying without ultrasound. Therefore, freezing pre-treatment and ultrasound application enhanced mass transfer during drying. However, significant changes in quality parameters of the final product were observed.

Keywords: beetroot, freezing, ultrasound, diffusional model, quality

1. INTRODUCTION

Beetroot contains polyphenols and two main betalain pigments: betaxanthins (yellow-orange) and betacyanins (red-violet) (Paciulli et al. 2016) which, apart from being colored, also have high antioxidant potential (Gengatharan et al. 2015). Although the most common preparations of beetroot are boiled or juice (Wootton-Beard and Ryan

2011), some new products have recently been studied, such as freeze and heat-dried beetroot (Figiel 2010; Kaleta and Górnicki 2010), dried powders processed by spray-drying, air-drying, or freeze-drying (Wruss et al. 2015) and juice microcapsules obtained by spray-drying (Janiszewska 2014). All these processes involve drying the sample in order to stabilize the product.

Convective drying is the most frequently used drying operation in the food and chemical industry (Samoticha et al. 2016). However, drying causes changes in the nutritional, physical and chemical properties of fruits, vegetables and their products (Onwude et al. 2016). These changes need to be carefully evaluated. Most of them, although observed at a macroscopic level, are caused by changes occurring at a microstructural/cellular level (Mayor et al. 2008). Therefore, microstructural changes also need to be studied when fruits and vegetables are dried. Different authors (Gokhale and Lele 2014; Székely et al. 2016; Nistor et al. 2017) have observed considerable changes in the microstructure and composition of bioactive compounds in beetroot depending on the drying conditions.

In order to intensify the drying process, many different pre-treatment methodologies have been proposed. Among them, freezing pre-treatment has been reported to enhance fruit and vegetable drying (Lewicki 2006). Freezing treatment (between −18 °C and −28 °C) prior to drying has been reported to reduce the drying time and, consequently, energy consumption, in the convective drying of green beans, carrots and potatoes at 70 °C (Eshtiaghi et al. 1994); rice micro-wave vibro-fluidized bed drying at 110-185 °C (Sripinyowanich and Noomhorm 2013); blueberries convective drying at 60-80 °C (Zielinska et al. 2015); carrots convective drying at 60 °C (Ando et al. 2016); among others. Freezing treatment might cause disruption of tissue structure which would lead to physico-chemical changes of the material, such as higher water absorption capacity (Lewicki 2006). At the same time, shortening the drying time reduces thermal exposure of the material, and consequently nutritional value could be better preserved. Studies of beetroot freezing before drying have not been found in the literature. However, osmotic dehydration pre-treatment and ultrasound pre-treatment have been reported to intensify beetroot convective drying at 60 and 70 ºC, respectively (Fijalkowska et al. 2015; Kowalski and Łechtańska 2015). Kowalski and Łechtańska (2015) observed that osmotic dehydration pre-treatment in 5 and 15% of NaCl solution for 30, 60 and 90 min shortened (20-32%) the beetroot drying time at 60 ºC and 1.2 m/s while presenting better quality parameters such as rehydration capacity, colour and betanin retention. Meanwhile, Fijalkowska et al. (2015) concluded that ultrasound pre-treatment using a frequency of 21 kHz during 10, 20 and 30 min reduced the drying time (5-9%), and the energy input (11-14%) and presented higher colour parameters and betalain content.

Ultrasound application in a drying system may overcome some of the limitations of convective drying by increasing the drying rate. Mainly at low temperature (less than 50 °C) (García-Pérez et al. 2006) and at low air velocities (less than 4 m/s) (Cárcel et al. 2007). Ultrasound application effects during hot-air drying of many products have been previously studied. The mechanical energy provided by the ultrasound application promotes alternating compressions and expansions which have a similar effect to that observed when a sponge is squeezed and released repeatedly: “sponge effect” (De la Fuente-Blanco et al. 2006). This “sponge effect” helps to release liquid from the inner part of a particle to its surface and promotes the suction of fluid from outside. The forces involved in this mechanism can be higher than the surface tension which maintains the water molecules inside the capillaries of the material, creating microscopic channels and facilitating the exchange of matter. Thus both internal and external resistances to mass transfer would be enhanced. No studies of the intensification of beetroot drying by ultrasound assistance have been found in the literature, although microwave intensification of beetroot drying has already been widely discussed (Kaur and Singh 2014; Nistor et al. 2017). Kaur and Singh (2014) observed that microwave finish drying at 540, 810 and 1080 W reduced beetroot drying time at 55, 65 and 75 ºC a maximum of 44% for 1080 W and 75 ºC. Moreover, these authors observed better rehydration properties, lesser colour degradation, stiff texture, maximum total soluble solids and safe water activity in final beetroot products. Nistor et al. (2017) observed that microwave (315 W) finish drying at 40 ºC enhanced the free convection beetroot drying at 50, 60 and 70 ºC (40- 52% of drying time reduction) and increased betacyanins, betaxanthins and polyphenol contents and % DPPH inhibition.

Therefore, the main objective of this study was to evaluate the influence of the freezing pre-treatment and the ultrasound application on the mass transfer in convective drying of beetroot cubes. For this purpose, the microstructure and also the drying curves using a diffusional model have been studied; likewise the changes in the betalain and total polyphenol contents, and in the antioxidant activity in the food matrix due to freezing pre-treatment and drying with ultrasound application have been evaluated.

NOMENCLATURE

AD	acoustic density (kW/m^3)
D_e	effective water diffusion coefficient (m^2/s)
dm	dry matter (kg)
h_m	external mass transfer coefficient (kg/m^2 s)
L	half of the length (m)
n	number of experimental data
MRE	mean relative error (%)
S_x	moisture content standard deviation (sample) (kg H_2O/kg dm)
S_{yx}	moisture content standard deviation (calculated) (kg H_2O/kg dm)
t	time (s)
Var	percentage of explained variance (%)
W	moisture content (kg H_2O/kg dm)
x,y,z	spatial coordinates (m)
ρ_{dm}	dry matter density (kg dm/m^3)

φ	relative humidity

Subscripts

0	initial
∞	drying air
cal	calculated
e	equilibrium
exp	experimental
l	local

2. MATERIALS AND METHODS

2.1. Sample processing

The beetroot (*Beta vulgaris* var. conditiva) used in this study, purchased in a local market, was selected on a range of 10.7 ± 0.9 °Brix, washed, peeled and cut into cubes (0.008m edge) from the center regions of the beetroot tissue and immediately processed. The initial average moisture content (W_0) was obtained by using the AOAC method No. 934.06 (AOAC 2006). Two sets of experiments were carried out. In set R, samples were immediately dried meanwhile in set F, samples were placed on a stainless steel load tree and frozen in a blast freezer (RDM051S, HIBER, Taiedo di Chions, Italy) at –20 °C (5.5 ± 0.1 °C/min freezing rate) prior to drying. Frozen samples were placed directly into the preheated drier without thawing.

The drying experiments were carried out in a convective drier assisted by ultrasound, which has already been described in a previous work (Cárcel et al. 2011). The equipment consisted of a pilot-scale convective drier with an aluminum cylindrical vibrating element (internal diameter 0.1 m, height 0.31 m and thickness 10 mm) working as the drying chamber where the load tree was placed. The cylinder was driven by a piezoelectric transducer (21.8 kHz); thus, the ultrasonic system was able to generate a high intensity ultrasonic field in the air medium with an average sound pressure of 154.3 ± 0.1 dB. The drier operated completely automatically. Air temperature and velocity were controlled using a PID algorithm, and samples were weighted at preset times by combining two pneumatic systems and a PLC (CQM41, Omron, Tokyo, Japan). The experiments were carried out at constant air velocity (1 m/s) and drying air temperature (40 °C), without (R0 and F0 samples) and with ultrasound at two different acoustic densities, 16.4 kW/m^3 (40 W) (R1 and F1 samples) and 26.7 kW/m^3 (65 W) (R2 and F2 samples). All the drying experiments were carried out, at least, in triplicate and extended until an 80% of sample weight loss was achieved.

2.2. Microstructural Analysis

Beetroot samples were prepared for light microscopy observation according to the methodology described by Eim et al. (2013), with minor modifications. Samples were fixed in formaldehyde (10%) followed by dehydration, embedded in paraffin (60 °C for 3 h), and sectioned into 4-5 μm sections by using a microtome (Finesse 325, Thermo Shandon, Cheshire, UK). The sections were stained with Periodic Acid–Schiff (PAS) and Hematoxilin Eosin (H-E) to visualize cell walls (Paciulli et al. 2015). The microstructural images were obtained using an optical microscope (BX41, Olympus, Tokyo, Japan) and a camera (DP71, Olympus, Tokyo, Japan) at 200x magnification.

2.3. Modelling

With the aim of obtaining a mathematical model representative of the moisture transport during the drying process, Fick’s second law was combined with the microscopic mass transfer balance and the process was considered to be isothermal. The governing equation for a differential element of cubic shape was formulated (Eq. 1) considering liquid diffusion to be the main transport mechanism.

$$D_e\left(\frac{\partial^2 W_l}{\partial x^2}+\frac{\partial^2 W_l}{\partial y^2}+\frac{\partial^2 W_l}{\partial z^2}\right)=\frac{\partial W_l}{\partial t} \tag{1}$$

A constant and effective diffusion coefficient (D_e), representative of the global transport process, might include molecular diffusion, liquid diffusion through the solid pores, vapor diffusion and all others factors which affect drying characteristics (Rodríguez et al. 2013). The governing equation (Eq. 1) could be solved considering as an initial condition, that the moisture distribution inside the solid was uniform at the beginning of the process (Eq. 2). As boundary conditions, moisture distribution symmetry (Eq. 3), and the external mass transfer at the solid surface (Eq. 4) were considered.

$$\left.W_{l(x,y,z)}\right|_{t=0}=W_0 \tag{2}$$

$$\left.\frac{\partial W_{l(x,y,z)}}{\partial x}\right|_{x=0}=\left.\frac{\partial W_{l(x,y,z)}}{\partial y}\right|_{y=0}\left.\frac{\partial W_{l(x,y,z)}}{\partial z}\right|_{z=0}=0 \tag{3}$$

$$\begin{gathered}
-D_e\rho_{dm}\left.\frac{\partial W_{l(x,y,z)}}{\partial x}\right|_{x=L}=h_m(\varphi_e-\varphi_\infty)\\
-D_e\rho_{dm}\left.\frac{\partial W_{l(x,y,z)}}{\partial y}\right|_{y=L}=h_m(\varphi_e-\varphi_\infty)\\
-D_e\rho_{dm}\left.\frac{\partial W_{l(x,y,z)}}{\partial z}\right|_{z=L}=h_m(\varphi_e-\varphi_\infty)
\end{gathered} \tag{4}$$

The sorption isotherm reported by Figiel (2010) and the psychometric data were considered to complete the model.

COMSOL Multiphysics® 5.1 (COMSOL Inc., Sweden) was used to solve the mathematical model, applying the finite elements method (FEM). After the mesh independence test, a domain composed of about 2650 quadratic triangular elements, resulting in about 3500 degrees of freedom was used. Matlab 2014a® (The Mathworks, Inc., Natick, USA) was used to develop the algorithm to identify both the effective diffusion (D_e) and the external mass transfer (h_m) coefficients from each drying curve through the minimization of the objective function (mean relative error) given by the Eq. 5.

$$MRE = \frac{100}{n} \sum_{i=1}^{n} \left| \frac{W_{exp_i} - W_{cal_i}}{W_{exp_i}} \right| \quad (5)$$

2.4. Bioactive compounds and antioxidant activity determinations

Raw (R), frozen (F) and dried samples without (R0 and F0) and with ultrasound application (R1, R2, F1 and F2) were analyzed to determine their betaxanthins (BXC), betacyanins (BCC) and total polyphenol (TPC) contents, and antioxidant activity (AA). Methanol extracts from the beetroot samples were prepared according to the methodology described by Heredia and Cisneros-Zevallos (2009) with some modifications. Both raw (R) and frozen (F) samples were used in their natural state as fresh vegetable. Samples were accurately weighed (~2 g) and 20 mL of methanol extraction solvent was added. The mixture was homogenized using Ultra-Turrax© (T25 Digital, IKA, Staufen, Germany) at 13,000 rpm for 1 min at 4 °C, and then the obtained solution was refrigerated overnight. Mixtures were centrifuged at 4,000 rpm for 10 min, and then filtered. The extracts were refrigerated at 4 °C until analysis. At least, six methanol extracts were prepared for each sample.

Betalain content was determined as betaxanthins (BXC) and betacyanins (BCC) content, separately, according to Stintzing et al. (2005). Absorbance measurements were carried out at 25 °C in a UV/Vis/NIR spectrophotometer (UV-2401PC, Shimadzu, Kyoto, Japan) at 476 and 535 nm, respectively. The betalain content was expressed as mg indicaxantin equivalent (IE)/g dm for BXC and mg betanin equivalent (BE)/g dm for BCC.

Total polyphenol content (TPC) was determined by means of the Folin-Ciocalteu assay according to Eim et al. (2013). The antioxidant activity (AA) was determined using FRAP, CUPRAC and ABTS methods according to González-Centeno et al. (2012). Absorbance measurements were carried out at 25 °C in a UV/Vis/NIR spectrophotometer (Thermo Scientific Multiskan Spectrum, Vantaa, Finland) at 745 (TPC), 593 (FRAP), 450 (CUPRAC) and 734 (ABTS) nm, and were correlated with standard curves (0-250 mg/L gallic acid for TPC and 0-400 mg/L trolox for AA). The results were expressed as mg of gallic acid equivalent (GAE)/g dm for the TPC, while the AA was expressed as mg trolox equivalent (TE)/g dm.

2.5. Statistical analyses

Statistical analyses were carried out using R© (GNU project) software. Data were averaged from replicates and reported as mean ± standard deviation. Two-factor analysis of variance (ANOVA) was applied to analyze the effects of both the freezing pre-treatment and the ultrasound application during drying on the betalain content, total polyphenol content and antioxidant activity. Means were compared by Tukey's test at $p<0.05$.

Additionally, the mean relative error (MRE, Eq. 5) and the percentage of explained variance (Var, Eq. 6) were used to evaluate the accuracy of the obtained simulation.

$$Var = \left[1 - \frac{S_{xy}^2}{S_y^2}\right] \cdot 100 \qquad (6)$$

3. RESULTS AND DISCUSSION

3.1. Microstructural Analysis

The study of the effect of pre-freezing treatment and of the use of ultrasound during drying on the microstructure of beetroot has been carried out by means of light microscopy. Due to its homogeneous pattern, parenchyma tissue was selected to observe changes and compare different treatments. The photographs of raw, pre-frozen and dried beetroots are shown in figure 1. The raw sample, which is shown in figure 1a, presented typical beetroot isodiametrical and polyhedral cells with few intercellular spaces as has been reported by Nayak et al. (2007). During drying one of the most important phenomena is cell shrinkage, which leads to a major modification in the structure of the product and allows the release of water (Ramos et al. 2004). Comparing figures 1a (raw sample) and 1c (dried sample) it can be seen how shrinkage took place in dried samples during drying at 40 °C and 1 m/s of air velocity.

Figure 1b shows the structure of the frozen beetroot sample (F) before drying. It can be observed that freezing pre-treatment caused disruptions and fissures in the beetroot tissue, similar to that reported on asparagus, zucchini and green beans frozen at –40 °C prior to boiling (Paciulli et al. 2015). Moreover, a freeze-thaw cycle seemed to promote cell collapse resulting in large intercellular spaces and the loss of cohesion, as has been observed on papaya tissue after the first freeze-thaw cycle at –25 °C and 4 °C (Phothiset and Charoenrein 2014).

Regarding ultrasound application, it can be seen in figures 1e and 1g that the use of acoustic densities of 16.4 and 26.7 kW/m^3 during drying contributed to disrupting the cellular structure, presenting slightly larger pores than in R0 samples. Moreover, the higher the acoustic density applied, the more disruption and larger pores were observed in samples. Similar effects were observed under the same drying conditions (at 40 °C and 1 m/s) by García-Pérez et al. (2012) in orange peel drying with acoustic density of 37 kW/m^3 and by Rodríguez et al. (2014) in apple drying with acoustic density of 30.8 kW/m^3. Both studies concluded that ultrasound application during drying produced an even more intense disruption than conventional drying creating micro-channels and making the water pathway easier.

Figure 1d shows the pre-frozen dried sample without ultrasound application. Notable cellular damage and irregular shapes in the cell structure of this sample can be observed, together with cell shrinkage due to the drying process. Finally, figures 1f and 1h show the pre-frozen dried sample with ultrasound application at the two acoustic densities tested. Those samples presented a sum of freezing, drying and ultrasound application effects previously described.

3.2. Drying kinetics

The initial moisture content of raw beetroot in this study, of 8.7 ± 0.1 kg/kg dm was within the range proposed in the literature by Kaleta and Górnicki (2010) (between 6 and 8 kg/kg dm) and by Figiel (2010) (10.2 kg/kg dm) for the same vegetable. No significant differences ($p>0.05$) were observed between the initial moisture content of raw and frozen samples, thus it was not significantly changed by the freezing pre-treatment, as has also been reported after the freezing at –20 °C of blueberries (Zielinska et al. 2015).

Figure 2 shows the experimental drying curves obtained for raw and pre-frozen beetroot cubes with and without ultrasound application at 40 °C and 1 m/s, from the initial moisture content down to ca 0.45 ± 0.02 kg/kg dm of final moisture content. The drying times for this final moisture content of the raw (R0) and pre-frozen (F0) sample when ultrasound was not applied (R0) were approximately of 5.4 and 3.0 h, respectively, thus drying time was 46% shorter, when the sample was pre-frozen. This suggests that the freezing pre-treatment led to an improvement in the water removal during the drying process. Zielinska et al. (2015) reported drying time reductions of 13 and 20% when pre-frozen (at –20 °C) blueberries were dried at 60 and 80 °C, respectively, compared to the raw sample. A similar reduction of drying time (40%) was observed when pre-frozen (at –20 °C) carrots were dried at 60 °C (Ando et al. 2016). When beetroot was osmotically (with 5 and 15% solutions of NaCl for 60 and 90 min) or ultrasonically (at 21 kHz for 10, 20 and 30 min) pre-treated, drying time reductions of 20-32% (drying at 60 ºC and 1.2 m/s) and 4.5-9% (drying at 70 ºC and 1.5 m/s) were observed, respectively (Fijalkowska et al. 2015; Kowalski and Łechtańska 2015).

When acoustic densities of 16.4 kW/m^3 (R1) and 26.7 kW/m^3 (R2) were applied, reductions of the drying time of 36 and 43% were observed, respectively, compared with the raw sample. It is difficult to analyze the effects of different ultrasonic devices because their efficiency is very dependent on the characteristics of the vibrating element. Thus, the comparison of drying experiments carried out with the same aluminum cylindrical vibrating element and air conditions (40 °C and 1 m/s) is more appropriate (Ozuna et al. 2011). When an acoustic density of 30.8 kW/m^3 was applied to carrot cubes drying, a drying time reduction of 30% was observed (Cárcel et al. 2011); in potato cubes drying, the application of 37 kW/m^3 caused a drying time reduction of 40% (Ozuna et al. 2011). All these time reductions were similar to those observed in the present work. Carrot, potato and beetroot could be considered “low porosity” products (their porosity values “Ɛ” are lower than 0.050) (Boukouvalas et al. 2006) and might be less-sensitive to the effects of the ultrasound application. The effect of ultrasound application on the mass transport has been linked to the alternative expansions and compressions produced in the material by ultrasonic waves, the “sponge effect” (De la Fuente-Blanco et al. 2006). Other products, like apple or eggplant (“medium-high porosity” products, their porosity values “Ɛ” are higher than 0.100) (Boukouvalas et al. 2006) seemed to be more sensitive to the “sponge effect” exhibiting reductions of 54 and 75%, respectively, at 37 kW/m^3 of acoustic density under the same air drying conditions (40 °C and 1 m/s) (Puig et al. 2012; Sabarez et al. 2012). According to Kaur and Singh (2014) and Nistor et al. (2017), when beetroot drying (at 50-70 ºC and 55-75 ºC, respectively) was intensified by microwave finish drying (at 540-1080 W and 315 W, respectively) drying time reductions of 44% and 40-52% were reported.

Similarly, ultrasound application during the drying of pre-frozen samples also caused a decrease in the drying time of 55% (F1) and 58% (F2) in comparison with the raw sample.

According to these results, both the freezing pretreatment and the ultrasound application (at 16.4 kW/m^3 and 26.7 kW/m^3) during drying enhanced the mass transfer and consequently reduced the drying time. Comparing with other combined methods, reductions in the drying time (11-39%) have been reported when pre-frozen rice (at –20 °C) was dried (110-185 °C) with micro-wave assistance (850 W) (Sripinyowanich and Noomhorm 2013).

In order to evaluate the existing drying periods, water flux (kg/kg dm m^2 s) was estimated and represented vs the average moisture content for all samples, as seen in figure 3. Here, no constant rate period was observed and all drying curves fell within the falling rate period except for the first moments of the frozen samples drying. This behavior of raw samples has also been reported by other authors in the convective drying of different fruits and vegetables, like eggplant (Puig et al. 2012) and orange peel (García-Pérez et al. 2012); among others. In the case of frozen samples, water flux was very low at the beginning of the process while these samples were thawing (induction period). Similar behavior has been reported for pre-frozen (at –30 °C) apple slices prior to drying at 65 °C and 1.2 m/s (Ramírez et al. 2011). During the first 4 min of the drying process, an increment in the mass flux was observed by these authors, as the surface temperature of apple slices increased. It can be also seen in figure 3 that the water flux was higher when samples were pre-frozen or/and ultrasound was applied during drying.

3.2.1. Modelling

In order to better study the effect of both the freezing pre-treatment and the ultrasound application on the mass transfer phenomenon, mathematical modeling was used as a tool for explaining and quantifying the observed enhancement of water removal during drying. A first attempt at modeling the drying curves was made assuming that the external resistance to mass transfer could be neglected, thus considering that the solid surface was at equilibrium with the drying air from the early stages of the drying process.

However, the simulation of the drying curves under these conditions did not provide satisfactory results (results not shown).

Therefore, both the external mass transfer (h_m) and the effective diffusion (D_e) coefficients were simultaneously identified by minimizing the differences between the experimental and simulated drying curves of the beetroot. The identified figures for these parameters (h_m and D_e) are summarized in table 1 for each drying experiment. As can be observed in this table, there were notable effects of both the freezing pre-treatment and the ultrasound application on the effective diffusion coefficient while only the ultrasound application affected the external mass transfer coefficient.

The identified h_m was of 2.18×10^{-4} kg/m^{2}s for R0 sample, similar to that for potato cubes drying at 40 °C and 1 m/s (2.03×10^{-4} kg/m^{2}s) (Ozuna et al. 2011). As expected, the freezing pre-treatment did not increase the h_m coefficient which was equal to that for the R0 sample. The external mass transfer coefficient is, in fact, a parameter that takes into account the conditions in the external resistance to mass transfer (the layer of fluid, air, which surrounds the sample undergoing drying). The case is different when ultrasound waves were applied. Here, ultrasound also influenced the external resistance and the h_m increased due to ultrasound application up to 2.79×10^{-4} kg/m^{2}s in R1 and F1 samples (when an acoustic density of 16.4 kW/m^3 was applied) and to 3.24×10^{-4} kg/m^{2}s in R2 and F2 samples (26.7 kW/m^3). Thus, compared with R0 and F0, increases of 28 and 49% respectively were observed. When acoustic densities of 18.5 and 37 kW/m^3 were applied during orange peel slabs drying at 40 °C and 1 m/s important increments on h_m were also observed (47 and 108%) (García-Pérez et al. 2012). These results would seem to indicate that the ultrasound application may induce decreases in the external resistance to the mass transfer probably due to pressure variations at the solid/gas interfaces, and therefore increasing the surface moisture evaporation rate (Rodríguez et al. 2014). Moreover, acoustic energy creates turbulences, oscillating velocities and microstreaming at the interfaces, which leads to a reduction of the boundary layer thickness (Gamboa-Santos et al. 2014). In conclusion, identified h_m figures for pre-frozen samples were equal to those for the respective raw samples, indicating that the freezing pre-treatment did not affect the external resistance to mass transfer during drying.

Although more experimentation needs to be done, the variation of the h_m coefficient with the acoustic density (AD) appeared to be linear with a determination coefficient of 0.99 (Ec. 7).

$$h_m = 3.95 \times 10^{-6} \cdot AD + 2.17 \times 10^{-4} \qquad r^2 = 0.998 \tag{7}$$

The identified D_e was of 3.07×10^{-10} m^2/s for R0 sample drying, which was in the range of those observed in carrot cubes and lemon peel slabs drying at 40 °C and 1m/s (1.20 and 4.95×10^{-10} m^2/s) (García-Pérez et al. 2009). The freezing pre-treatment caused a considerable increase in the D_e up to 7.93×10^{-10} m^2/s (158% increment in comparison to the R0 sample) probably due to the cellular tissue damage which improved the water transfer throughout the solid. This effect was also reported for pre-frozen (at –30 °C) apple slices drying at 65 °C and 1.2 m/s where identified effective diffusivity increased 30% in comparison with the raw sample (Ramírez et al. 2011). This parameter (D_e) also increased due to the ultrasound application up to 4.92×10^{-10} m^2/s in R1 sample (16.4 kW/m^3) and 5.32×10^{-10} m^2/s in R2 sample (26.7 kW/m^3) thus, compared with R0, increases of 60 and 73% respectively, were observed. When acoustic densities of 16 and 25 kW/m^3 were applied during lemon peel slabs drying at 40 °C and 1 m/s, similar increases in D_e were observed (49 and 99%) (García-Pérez et al. 2009). When samples were pre-frozen and dried with ultrasound application, D_e increased up to 9.32×10^{-10} m^2/s in F1 sample (16.4 kW/m^3) and 9.54×10^{-10} m^2/s in F2 sample (26.7 kW/m^3). Thus, compared with the R0 sample, increases of 204 and 211% respectively, were observed. No significant differences (p>0.05) were observed between identified D_e figures for R1 and R2, and for F1 and F2. These results indicated that not only the freezing pre-treatment caused increases in D_e, but also the ultrasound application.

By using the identified D_e and h_m figures, the drying curves were simulated. In order to evaluate the simulation, the predicted moisture content has been represented vs the experimental one for all the experiments in figure 4. This figure also shows the regression analysis and the prediction boundaries at 95% confidence. As can be seen in this figure, a good match between both groups of data (predicted and experimental) was obtained for both raw and frozen samples dried without or with ultrasound application. The correctness of the simulation was corroborated by the regression analysis. The y-intercept and the slope figures were close to zero and to unity, respectively, and the coefficient of determination, which describes the good correlation of the predicted concentrations with their experimental values, was higher than 0.99. To mathematically evaluate the simulation, the mean relative error (MRE) (Eq. 5) and the percentage of explained variance (Var) (Eq. 6) were calculated for each experiment. Results are also shown in table 1. As can be seen, MRE was lower than 5% and the Var was higher than 99.6% for the simulation of all the experiments. It could be concluded from both figure 4 and table 1, that the drying curves of beetroot were satisfactorily simulated using the proposed model.

3.3. Bioactive compounds and antioxidant activity determinations

The effects of processing on the bioactive compounds of beetroot, betaxanthins (BXC), betacyanins (BCC) and total polyphenol (TPC) contents, and antioxidant activity (AA) were determined in raw and pre-frozen samples before and after convective drying. To achieve a more complete view, three methods were used to evaluate the antioxidant activity (AA) of the samples: FRAP, CUPRAC and ABTS. Due to the fact that each method is based on a different chemical system and/or reaction, different results of AA could be expected depending on the method used (González-Centeno et al. 2012). The selection of different methods allows a better understanding of the wide variety and range of action of antioxidant compounds present in beetroots.

Figures 5 and 6 show the bioactive compounds content and the AA of raw and pre-frozen beetroot cubes before and after drying with and without ultrasound application, respectively. According to the two-way ANOVA, the effects of freezing pre-treatment and ultrasound application exhibited were significant ($p<0.05$) on BXC, BCC, TPC and AA (FRAP, CUPRAC and ABTS methods). The interaction between these factors was also significant ($p<0.05$). Therefore, Tukey's multiple range test analysis was carried out considering all samples simultaneously. The results of the Tukey's multiple range test analysis are also shown with different lowercase letters in the same determination when samples are significantly different at a significance level of $p<0.05$.

Initial values of BXC, BCC, TPC and AA according to FRAP, CUPRAC and ABTS methods in raw beetroot (R) were of 2.34 ± 0.03 mg IE/g dm, 2.34 ± 0.17 mg BE/g dm, 6.5 ± 0.2 mg GAE/g dm and 13.4 ± 0.4, 31.5 ± 0.9 and 19.1 ± 1.0 mg TE/g dm, respectively. These initial values were in the range of those proposed by Wruss et al. (2015) for seven beetroots varieties: 1.5 ± 0.2-2.4 ± 0.3 mg IE/g dm for BXC, 2.3 ± 0.2-3.9 ± 0.5 mg BE/g dm for BCC and 4.1 ± 0.7-6.3 ± 0.9 mg GAE/g dm for TPC except for the initial value of AA according to FRAP method which was lower than the range proposed by Wruss et al. (2015): 21.1 ± 4.9-45.0 ± 7.5 mg TE/g dm. BXC, BCC, TPC and AA according to FRAP method of frozen samples significantly ($p<0.05$) increased by 57, 57, 16 and 37% compared to the raw sample (R). Freezing pre-treatment seemed to affect the beetroot cell structure accelerating the reaction between different substances to generate free forms. Similar behavior has been previously observed in the TPC (59% increase) of black garlic after freezing pre-treatment at –18 °C (Li et al. 2015) and in the TPC and AA (FRAP method) (30 and 18% increase) of broccoli florets after freezing at –26 °C (Cai et al. 2016). However, no significant ($p>0.05$) changes (less than

4%) were observed in the AA of the frozen sample (F) in comparison with the raw sample (R) according to CUPRAC and ABTS methods.

After the drying process, BXC, BCC, TPC and AA of the R0 sample decreased in comparison with the initial values (R sample) by 47%, 54%, 10% and 13 ± 5% (average of FRAP, CUPRAC and ABTS results), respectively. The convective drying process caused an intensive oxidation that occurred during the long exposure to hot air. Betacyanins and betaxanthins are temperature sensitive pigments as has been demonstrated previously by Fernández-López and Almela (2001) with prickly pear fruits and by Ravichandran et al. (2013), Gokhale and Lele (2014) and Székely et al. (2016) with beetroot processing. Moreover, the convective drying process seemed to destroy beetroot antioxidant compounds as reported by Figiel (2010) when beetroot was dried at 60 °C and 1.8 m/s. This author observed that beetroot antioxidant activity (measured by FRAP method) decreased by 29% after the drying process, compared with the raw sample. Regarding the pre-frozen sample after drying without ultrasound application (F0), BXC, BCC, TPC and AA decreased in comparison with the initial values (R sample) by 58%, 61%, 28% and 47 ± 8% (average of FRAP, CUPRAC and ABTS results), respectively. No significant differences ($p>0.05$) were observed in the final betaxanthins and betacyanins contents between R0 and F0 samples, thus, the betalain content of beetroot cubes after drying was not modified when samples were pre-frozen before drying. Comparing with other pre-treatments, according to Kowalski and Łechtańska (2015) and Fijalkowska et al. (2015), osmotically (with 5 and 15% solutions of NaCl for 30, 60 and 90 min) or ultrasonically (at 21 kHz for 10, 20 and 30min) pre-treated dried beetroot presented higher or similar betalain content. However, TPC and AA, according to FRAP, CUPRAC and ABTS methods of the pre-frozen sample (F0), significantly decreased ($p<0.05$) in comparison with the R0 sample.

Significant effects ($p<0.05$) of ultrasound during drying on the BXC, BCC, TPC and AA of beetroot were observed in the case of the raw samples. When ultrasound energy was applied at 16.4 kW/m^3 (R1 sample) and 26.7 kW/m^3 (R2 sample) of acoustic density, BXC, BCC, TPC and AA decreased by 68-72%, 73-81%, 43-51% and 39-55% (average of FRAP, CUPRAC and ABTS results), respectively. No significant differences ($p>0.05$) were observed between the BXC and BCC of R1 and R2 samples. However, significant differences ($p<0.05$) between R1 and R2 samples with regard to the TPC and the AA were observed. Thus the ultrasound application caused higher TPC and AA losses, mainly when the highest acoustic density (26.7 kW/m^3) was applied. These results could be related to the cellular damage induced by the combination of the drying temperature and the ultrasound application. Similar behavior was observed in drying apple at 70 °C and 1 m/s of air velocity, where TPC loss was higher (39% of loss) when the higher acoustic density was applied (30.8 kW/m^3) (Rodríguez et al. 2014). Comparing this to drying intensification (at 50-70 ºC) by microwave finish drying (at 315 W and 40 ºC), Nistor et al. (2017) reported higher (between 4 and 295% increases compared with conventional dried sample) TPC, BXC, BCC and AA (measured by DPPH method), probably due to the shortened drying time which reduced thermal oxidation.

Similarly, in the case of pre-frozen samples (F1 and F2), the use of ultrasound caused significant effects ($p<0.05$). Higher BXC, BCC, TPC and AA decreases in comparison with the initial values (R sample) were observed when ultrasound energy was applied to drying of pre-frozen samples at 16.4 kW/m^3 (F1 sample) and 26.7 kW/m^3 (F2 sample) of acoustic density: 71-76%, 70-79%, 56-50% and 55 ± 2-56 ± 7% (average of FRAP, CUPRAC and ABTS results), respectively. No significant differences ($p>0.05$) were observed between the BXC and BCC of F1 and F2 samples, although significant differences ($p<0.05$) between F1 and F2 samples with regard to the TPC and AA were observed. TPC and AA (FRAP method) were significantly higher ($p<0.05$) in F2 sample than in F1 sample. Thus, when samples were pre-frozen, TPC, BXC, BCC and AA (FRAP method) were preserved when drying was carried out at the highest acoustic density tested: 26.7 kW/m^3, probably due to the reduction of hot air exposure time, since polyphenols, betaxanthins and betacyanins are temperature sensitive compounds. Similar behavior has been observed for beetroot cubes dried by vacuum-microwave method at 60 ºC and 1.8 m/s air velocity when power of 240 and 480 W were applied. Antioxidant activity (measured by FRAP method) was preserved when vacuum-microwave power was applied during drying because thermal degradation was decreased due to a reduction in hot air exposure time (Figiel 2010). However, higher losses of AA were observed in F2 than in F1 according to the CUPRAC and ABTS methods.

4. CONCLUSIONS

Important microstructural changes disruptions and fissures were observed in beetroot tissue after freezing pre-treatment and also when samples were dried, especially when drying was carried out by applying ultrasound. Thus, drying time of beetroot decreased when ultrasound was applied during drying (36-43%) and also when samples were frozen before drying without (46%) or with ultrasound application (55-58%). Thus, both pre-freezing and ultrasound application during drying enhanced the mass transfer and reduced the drying time. By using a diffusional model, and taking into account both the external and the internal mass transfer resistances, the drying curves with and without ultrasound application, of raw and pre-frozen beetroot cubes were satisfactorily simulated (average MRE was of 2.9 ± 0.9%). Ultrasound application during drying induced considerable increases in both the external mass transfer (28-49%) and the effective diffusion (60-73%) coefficients. Meanwhile, freezing pre-treatment induced increases only in the internal coefficient (158%). Therefore, not only freezing pre-treatment but also ultrasound application was suitable for the intensification of the drying kinetics of beetroot. With regard to the effects of processing on the bioactive compounds of beetroot, freezing caused significant ($p<0.05$) increases, probably due to the release of free forms of active compounds from the food matrix, meanwhile drying had the opposite effect. Moreover, when ultrasound was applied during drying, decreases were higher. Thus, although freezing pre-treatment and ultrasound application during drying could be used to increase the mass transfer rate, processing can affect the stability and availability of the bioactive compounds.

5. ACKNOWLEDGMENTS

The authors would like to acknowledge the INIA for the financial support (RTA2015-00060-C04-03 and RTA2015-00060-C04-02 projects) and the Spanish Government (MINECO) for the BES-2013-064131 fellowship.

6. REFERENCES

Ando, Y., Maeda, Y., Mizutani, K., Wakatsuki, N., Hagiwara, S. & Nabetani, H. (2016). Impact of blanching and freeze-thaw pretreatment on drying rate of carrot roots in relation to changes in cell membrane function and cell wall structure. LWT - Food Science and Technology, 71, 40-46.

AOAC (2006). Moisture in dried fruits. 934.06. *Association of Analytical Communities, 16th ed. Maryland.*

Boukouvalas, C. J., Krokida, M., Maroulis, Z. & Marinos-Kouris, D. (2006). Density and porosity: Literature data compilation for foodstuffs. International Journal of Food Properties, 9(4), 715-746.

Cai, C., Miao, H., Qian, H., Yao, L., Wang, B. & Wang, Q. (2016). Effects of industrial pre-freezing processing and freezing handling on glucosinolates and antioxidant attributes in broccoli florets. Food Chemistry, 210, 451-456.

Cárcel, J. A., García-Pérez, J. V., Riera, E. & Mulet, A. (2007). Influence of high-intensity ultrasound on drying kinetics of persimmon. Drying Technology, 25(1), 185-193.

Cárcel, J. A., García-Pérez, J. V., Riera, E. & Mulet, A. (2011). Improvement of convective drying of carrot by applying power ultrasound—Influence of mass load density. Drying Technology, 29(2), 174-182.

De la Fuente-Blanco, S., Riera-Franco de Sarabia, E., Acosta-Aparicio, V. M., Blanco-Blanco, A. & Gallego-Juárez, J. A. (2006). Food drying process by power ultrasound. Ultrasonics, 44, Supplement, e523-e527.

Eim, V. S., Urrea, D., Rosselló, C., García-Pérez, J. V., Femenia, A. & Simal, S. (2013). Optimization of the drying process of carrot (*Daucus carota* v. Nantes) on the basis of quality criteria. Drying Technology, 31(8), 951-962.

Eshtiaghi, M. N., Stute, R. & Knorr, D. (1994). High-pressure and freezing pretreatment effects on drying, rehydration, texture and color of green beans, carrots and potatoes. Journal of Food Science, 59(6), 1168-1170.

Fernández-López, J. A. & Almela, L. (2001). Application of high-performance liquid chromatography to the characterization of the betalain pigments in prickly pear fruits. Journal of Chromatography A, 913(1), 415-420.

Figiel, A. (2010). Drying kinetics and quality of beetroots dehydrated by combination of convective and vacuum-microwave methods. Journal of Food Engineering, 98(4), 461-470.

Fijalkowska, A., Nowacka, M. & Witrowa-rajchert, D. (2015). Effect of ultrasound waves on drying process and selected properties of beetroot tissue. Food Science Technology Quality, 2(99), 138-149.

Gamboa-Santos, J., Montilla, A., Cárcel, J. A., Villamiel, M. & Garcia-Perez, J. V. (2014). Air-borne ultrasound application in the convective drying of strawberry. Journal of Food Engineering, 128, 132-139.

García-Pérez, J. V., Cárcel, J. A., Riera, E. & Mulet, A. (2009). Influence of the applied acoustic energy on the drying of carrots and lemon peel. Drying Technology, 27(2), 281-287.

García-Pérez, J. V., Ortuño, C., Puig, A., Cárcel, J. A. & Perez-Munuera, I. (2012). Enhancement of water transport and microstructural changes induced by high-intensity ultrasound application on orange peel drying. Food and Bioprocess Technology, 5(6), 2256-2265.

García-Pérez, J. V., Rosselló, C., Cárcel, J., De la Fuente, S. & Mulet, A. (2006) Effect of air temperature on convective drying assisted by high power ultrasound. Defect and Diffusion Forum, Trans Tech Publ, vol 258, 563-574.

Gengatharan, A., Dykes, G. A. & Choo, W. S. (2015). Betalains: Natural plant pigments with potential application in functional foods. LWT - Food Science and Technology, 64(2), 645-649.

Gokhale, S. V. & Lele, S. S. (2014). Betalain content and antioxidant activity of beta vulgaris: Effect of hot air convective drying and storage. Journal of Food Processing and Preservation, 38(1), 585-590.

González-Centeno, M. R., Jourdes, M., Femenia, A., Simal, S., Rosselló, C. & Teissedre, P.-L. (2012). Proanthocyanidin composition and antioxidant potential of the stem winemaking byproducts from 10 different grape varieties (*Vitis vinifera* L.). Journal of Agricultural and Food Chemistry, 60(48), 11850-11858.

Heredia, J. B. & Cisneros-Zevallos, L. (2009). The effects of exogenous ethylene and methyl jasmonate on the accumulation of phenolic antioxidants in selected whole and wounded fresh produce. Food Chemistry, 115(4), 1500-1508.

Janiszewska, E. (2014). Microencapsulated beetroot juice as a potential source of betalain. Powder Technology, 264, 190-196.

Kaleta, A. & Górnicki, K. (2010). Some remarks on evaluation of drying models of red beet particles. Energy Conversion and Management, 51(12), 2967-2978.

Kaur, K. & Singh, A. (2014). Drying kinetics and quality characteristics of beetroot slices under hot air followed by microwave finish drying. African Journal of Agricultural Research, 9(12), 1036-1044.

Kowalski, S. J. & Łechtańska, J. M. (2015). Drying of red beetroot after osmotic pretreatment: Kinetics and quality considerations. Chemical and Process Engineering, 36(3), 345-354.

Lewicki, P. P. (2006). Design of hot air drying for better foods. Trends in Food Science & Technology, 17(4), 153-163.

Li, N., Lu, X., Pei, H. & Qiao, X. (2015). Effect of freezing pretreatment on the processing time and quality of black garlic. Journal of Food Process Engineering, 38(4), 329-335.

Mayor, L., Pissarra, J. & Sereno, A. (2008). Microstructural changes during osmotic dehydration of parenchymatic pumpkin tissue. Journal of Food Engineering, 85(3), 326-339.

Nayak, C. A., Suguna, K., Narasimhamurthy, K. & Rastogi, N. K. (2007). Effect of gamma irradiation on histological and textural properties of carrot, potato and beetroot. Journal of Food Engineering, 79(3), 765-770.

Nistor, O.-V., Seremet, L., Andronoiu, D. G., Rudi, L. & Botez, E. (2017). Influence of different drying methods on the physicochemical properties of red beetroot (*Beta vulgaris* L. var. Cylindra). Food Chemistry, 236, 59-67.

Onwude, D. I., Hashim, N. & Chen, G. (2016). Recent advances of novel thermal combined hot air drying of agricultural crops. Trends in Food Science & Technology, 57, 132-145.

Ozuna, C., Cárcel, J. A., García-Pérez, J. V. & Mulet, A. (2011). Improvement of water transport mechanisms during potato drying by applying ultrasound. Journal of the Science of Food and Agriculture, 91(14), 2511-2517.

Paciulli, M., Ganino, T., Pellegrini, N., Rinaldi, M., Zaupa, M., Fabbri, A. & Chiavaro, E. (2015). Impact of the industrial freezing process on selected vegetables — Part I. Structure, texture and antioxidant capacity. Food Research International, 74, 329-337.

Paciulli, M., Medina-Meza, I. G., Chiavaro, E. & Barbosa-Cánovas, G. V. (2016). Impact of thermal and high pressure processing on quality parameters of beetroot (*Beta vulgaris* L.). LWT - Food Science and Technology, 68, 98-104.

Phothiset, S. & Charoenrein, S. (2014). Effects of freezing and thawing on texture, microstructure and cell wall composition changes in papaya tissues. Journal of the Science of Food and Agriculture, 94(2), 189-196.

Puig, A., Pérez-Munuera, I., Cárcel, J., Hernando, I. & García-Pérez, J. (2012). Moisture loss kinetics and microstructural changes in eggplant (*Solanum melongena* L.) during conventional and ultrasonically assisted convective drying. Food and Bioproducts Processing, 90(4), 624-632.

Ramírez, C., Troncoso, E., Muñoz, J. & Aguilera, J. M. (2011). Microstructure analysis on pre-treated apple slices and its effect on water release during air drying. Journal of Food Engineering, 106(3), 253-261.

Ramos, I. N., Silva, C. L. M., Sereno, A. M. & Aguilera, J. M. (2004). Quantification of microstructural changes during first stage air drying of grape tissue. Journal of Food Engineering, 62(2), 159-164.

Ravichandran, K., Saw, N. M. M. T., Mohdaly, A. A. A., Gabr, A. M. M., Kastell, A., Riedel, H., Cai, Z., Knorr, D. & Smetanska, I. (2013). Impact of processing of red beet on betalain content and antioxidant activity. Food Research International, 50(2), 670-675.

Rodríguez, Ó., Eim, V. S., Simal, S., Femenia, A. & Rosselló, C. (2013). Validation of a difussion model using moisture profiles measured by means of TD-NMR in apples (*Malus domestica*). Food and Bioprocess Technology, 6(2), 542-552.

Rodríguez, Ó., Santacatalina, J. V., Simal, S., Garcia-Perez, J. V., Femenia, A. & Rosselló, C. (2014). Influence of power ultrasound application on drying kinetics of apple and its antioxidant and microstructural properties. Journal of Food Engineering, 129, 21-29.

Sabarez, H. T., Gallego-Juárez, J. A. & Riera, E. (2012). Ultrasonic-assisted convective drying of apple slices. Drying Technology, 30(9), 989-997.

Samoticha, J., Wojdyło, A. & Lech, K. (2016). The influence of different the drying methods on chemical composition and antioxidant activity in chokeberries. LWT - Food Science and Technology, 66, 484-489.

Sripinyowanich, J. & Noomhorm, A. (2013). Effects of freezing pretreatment, microwave-assisted vibro-fluidized bed drying and drying temperature on instant rice production and quality. Journal of Food Processing and Preservation, 37(4), 314-324.

Stintzing, F. C., Herbach, K. M., Mosshammer, M. R., Carle, R., Yi, W., Sellappan, S., Akoh, C. C., Bunch, R. & Felker, P. (2005). Color, betalain pattern, and antioxidant properties of cactus pear (*Opuntia spp.*) clones. Journal of Agricultural and Food Chemistry, 53(2), 442-451.

Székely, D., Illés, B., Stéger-Máté, M. & Monspart-Sényi, J. (2016). Effect of drying methods for inner parameters of red beetroot (*Beta vulgaris* L.). Acta Universitatis Sapientiae, Alimentaria, 9(1), 60-68.

Wootton-Beard, P. C. & Ryan, L. (2011). A beetroot juice shot is a significant and convenient source of bioaccessible antioxidants. Journal of Functional Foods, 3(4), 329-334.

Wruss, J., Waldenberger, G., Huemer, S., Uygun, P., Lanzerstorfer, P., Müller, U., Höglinger, O. & Weghuber, J. (2015). Compositional characteristics of commercial beetroot products and beetroot juice prepared from seven beetroot varieties grown in Upper Austria. Journal of Food Composition and Analysis, 42, 46-55.

Zielinska, M., Sadowski, P. & Błaszczak, W. (2015). Freezing/thawing and microwave-assisted drying of blueberries (*Vaccinium corymbosum* L.). LWT - Food Science and Technology, 62(1, Part 2), 555-563.

Figure captions

Fig. 1 Light microscope photographs of raw (R), pre-frozen (F) and dried beetroot cubes (40 °C and 1 m/s), without (0) and with ultrasound application at 16.4 kW/m^3 (1) and 26.7 kW/m^3 (2). Legend: is=intercellular spaces, s=shrinkage, f=fissure, d=disruptions, m=micro-channels

Fig. 2 Drying curves of raw (R) and pre-frozen (F) beetroot cubes (40 °C and 1 m/s), without (0) and with ultrasound application at 16.4 kW/m^3 (1) and 26.7 kW/m^3 (2). Average value ± standard deviation

Fig. 3 Variation of mass flux vs average moisture content during convective air-drying (40 °C, 1 m/s) of raw (R) and pre-frozen (F) beetroot cubes without (0) and with ultrasound application at 16.4 kW/m^3 (1) and 26.7 kW/m^3 (2). Average value ± standard deviation

Fig. 4 Predicted vs. experimental average moisture content. Drying experiments carried out with raw (R) and pre-frozen (F) beetroot cubes (40 °C and 1 m/s), without (0) and with ultrasound application at 16.4 kW/m^3 (1) and 26.7 kW/m^3 (2)

Fig. 5 Total polyphenol (a), betaxanthins (b) and betacyanins (c) contents (mg GAE or IE or BE/g dm) of raw (R;---), pre-frozen (F;—) and dried (40 °C and 1 m/s) beetroot cubes, without (0) and with ultrasound application at 16.4 kW/m^3 (1) and 26.7 kW/m^3 (2). Average value ± standard deviation. Means with different letter for total polyphenol, betaxanthins or betacyanins contents show significant differences according to Tukey's test ($p<0.05$)

Fig. 6 Antioxidant activity (AA) (mg TE/g dm) determined by FRAP (a), CUPRAC (b) and ABTS (c) methods for samples of raw (R;---), pre-frozen (F;—) and dried (40 °C and 1 m/s) beetroot cubes without (0) and with ultrasound application at 16.4 kW/m^3 (1) and 26.7 kW/m^3 (2). Average value ± standard deviation. Means with different letter for antioxidant activity show significant differences according to Tukey's test ($p<0.05$)

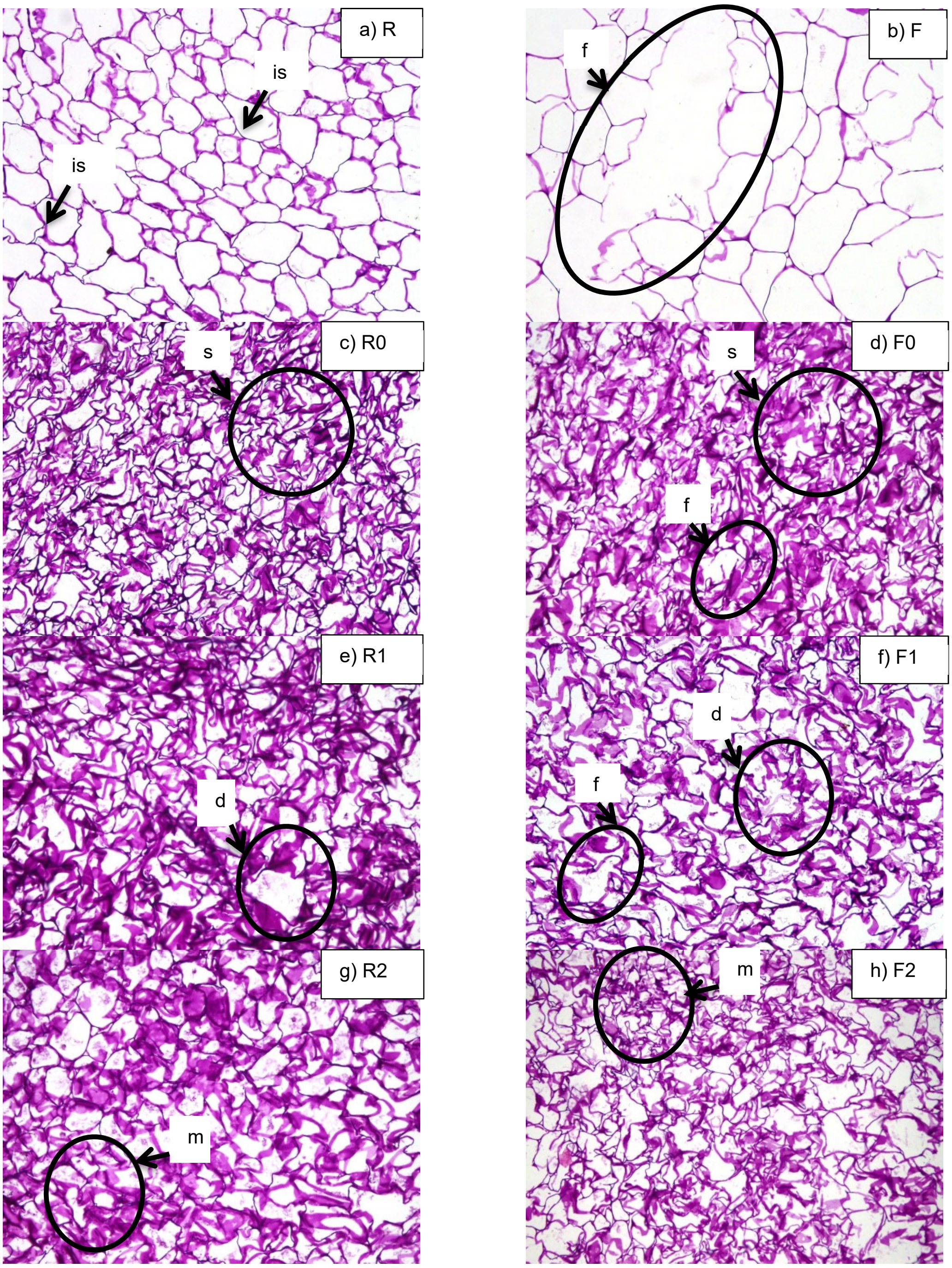
a) R
is
is
b) F
f
c) R0
s
d) F0
s
f
e) R1
d
f) F1
d
f
g) R2
m
h) F2
m

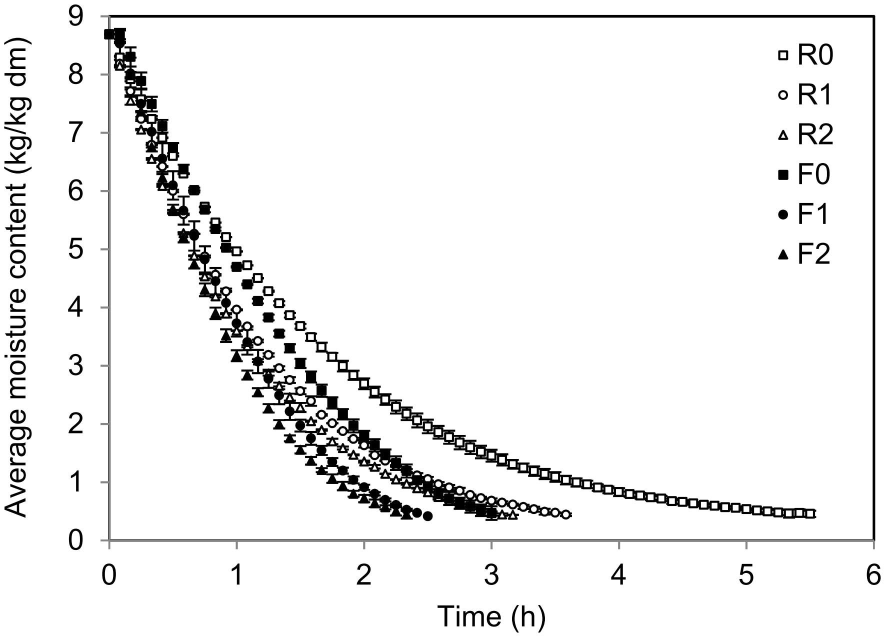
Average moisture content (kg/kg dm)
Time (h)
0
1
2
3
4
5
6
7
8
9
0
1
2
3
4
5
6
R0
R1
R2
F0
F1
F2

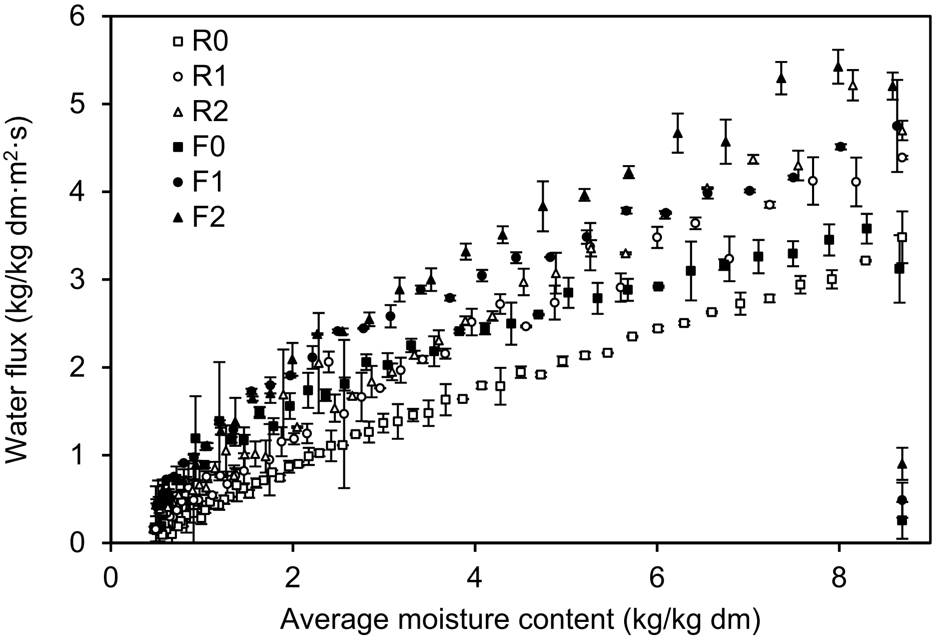
Water flux (kg/kg dm·m^2·s)
Average moisture content (kg/kg dm)
0
1
2
3
4
5
6
0
2
4
6
8
R0
R1
R2
F0
F1
F2

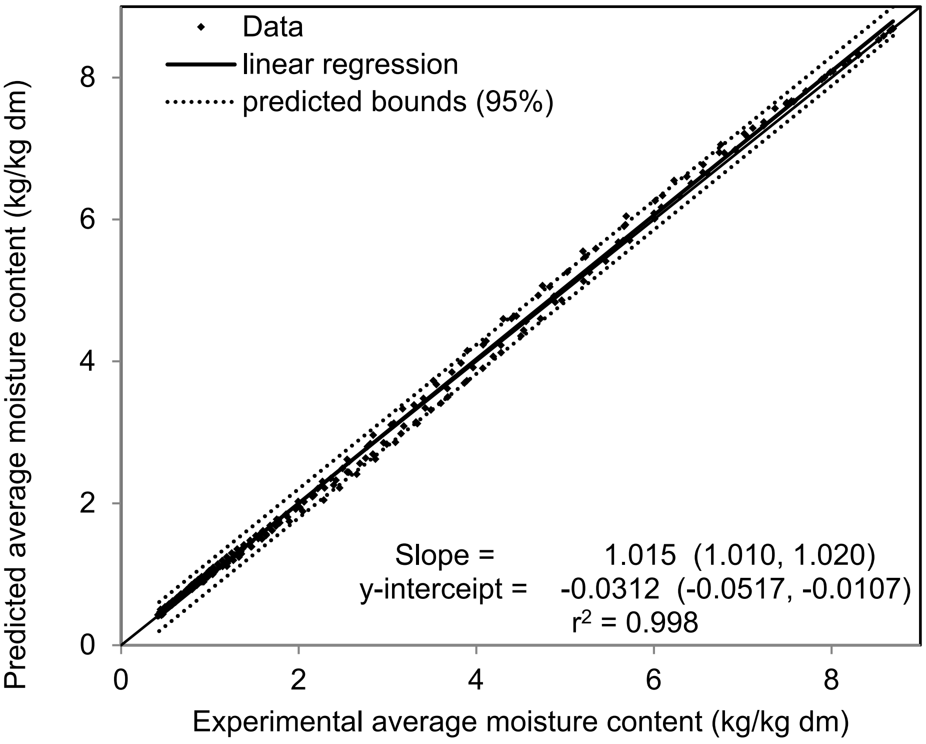
Data
linear regression
predicted bounds (95%)
Slope = 1.015 (1.010, 1.020)
y-interceipt = -0.0312 (-0.0517, -0.0107)
r2 = 0.998
Predicted average moisture content (kg/kg dm)
Experimental average moisture content (kg/kg dm)
0
2
4
6
8
0
2
4
6
8

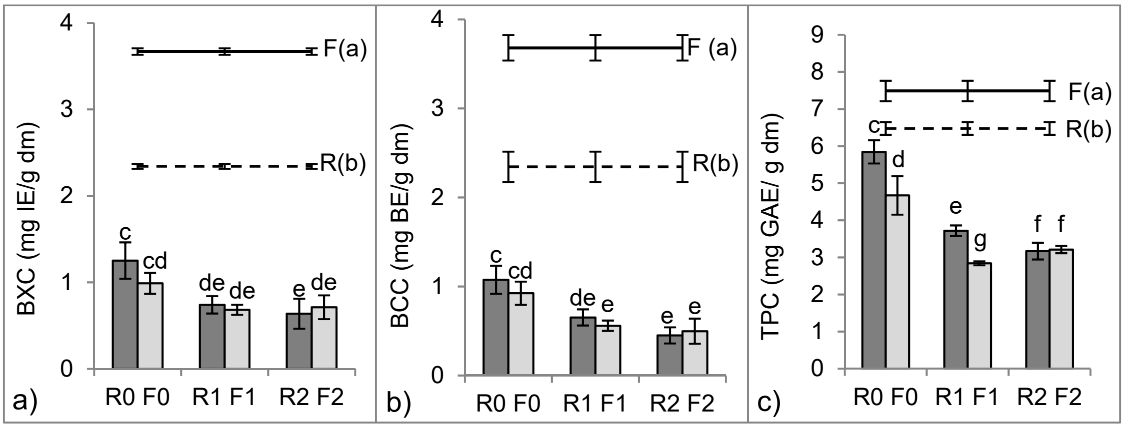
a)
BXC (mg IE/g dm)
0
1
2
3
4
F(a)
R(b)
c
cd
de
de
e
de
R0 F0
R1 F1
R2 F2
b)
BCC (mg BE/g dm)
0
1
2
3
4
F (a)
R(b)
c
cd
de
e
e
e
R0 F0
R1 F1
R2 F2
c)
TPC (mg GAE/ g dm)
0
1
2
3
4
5
6
7
8
9
F(a)
R(b)
c
d
e
g
f
f
R0 F0
R1 F1
R2 F2

Table 1. Identified figures for the external mass transfer (h_m) and the effective diffusion (D_e) coefficients, mean relative error (MRE) and percentage of explained variance (Var) obtained by comparison between the experimental and simulated drying curves of beetroot at 40 °C and 1 m/s. Average value ± standard deviation. Means with different superscript letter for the external mass transfer (h_m) and the effective diffusion (D_e) coefficients showed significant differences according to Tukey's test ($p<0.05$)

DRYING			$h_m \cdot 10^4$ (kg/m^{2}s)	$D_e \cdot 10^{10}$ (m^2/s)	MRE (%)	Var (%)
Without Ultrasound	Raw	R0	2.18 ± 0.03^a	3.07 ± 0.13^d	3.0±0.2	99.9±0.1
	Frozen	F0		7.93 ± 0.40^b	2.8±0.2	99.9±0.1
Ultrasound (16.4 kW/m^3)	Raw	R1	2.79 ± 0.04^b	4.92 ± 0.24^c	1.8±0.1	99.9±0.1
	Frozen	F1		9.32 ± 0.34^a	2.3±0.1	99.9±0.1
Ultrasound (26.7 kW/m^3)	Raw	R2	3.24 ± 0.04^c	5.32 ± 0.26^c	4.7±0.3	99.7±0.1
	Frozen	F2		9.54 ± 0.37^a	2.6±0.2	99.9±0.1